Electronic Supplementary Material (ESI) for Physical Chemistry Chemical Physics.

Supplementary material: Shell-Dependent Photofragmentation Dynamics of a Heavy-Atom-Containing Bifunctional Nitroimidazole Radiosensitizer

Lassi Pihlava,[1] Pamela H.W. Svensson,[2] Edwin Kukk,[1] Kuno Kooser,[3] Emiliano De Santis,[4] Arvo Tõnisoo,[3] Tanel Käämbre,[3] Tomas André,[2] Tomoko Akiyama,[2] Lisa Hessenthaler,[2] Flavia Giehr,[2] Olle Björneholm,[2] Carl Caleman,[2,5] and Marta Berholts[3]

[1]*Department of Physics and Astronomy, University of Turku, FI-20014 Turku, Finland*

[2]*Department of Physics and Astronomy, University of Uppsala, SE-75120 Uppsala, Sweden*

[3]*Institute of Physics, University of Tartu, W. Ostwald 1, EST-50411, Tartu, Estonia*

[4]*Department of Chemistry – BMC, University of Uppsala, SE-75123 Uppsala, Sweden*

[5]*Center for Free-Electron Laser Science, DESY, DE-22607 Hamburg, Germany*

In this supplementary information, we explain our ion transmission correction procedure and give the estimated transmissions in Table SI. We also present the photoelectron spectra measured during the PEPIPICO experiments (see Fig. S1, Fig. S2, and Fig. S3). Fig. S4 shows two additional fragmentation pathways simulated for $BrINim^{2+}$.

We applied the following method to estimate the ion transmission and correct for the ion loss in coincident TOF mass spectra. We extracted the three-dimensional momentum vector for each ion using the flight time and the hit position coordinate on the position-sensitive detector event by event. The x- and y-components of the momentum $\vec{p}$ were obtained by calculating the initial velocity in those directions based on the hit position and the flight time. The z-component - along the TOF spectrometer - was estimated from the difference between the ion's flight time and the nominal flight time (no initial velocity in the z-direction), and the acceleration of the ion in the interaction region. The ions form an origo-centered sphere in momentum space. To analyze the ion intensity, we projected them onto the p_{yz} plane and divided the momentum circle into sectors. Since the photon beam is in the x-direction, the ions are less focused in p_x and more focused in p_y, making p_x less suitable for correcting ion loss. However, the p_{xy} and p_{xz} planes were used to ensure that the momentum space was centered properly. To estimate the ion transmission for a particular m/z, we assume that (i) the momentum distribution is isotropic and (ii) all ions in the most populated sector are detected. Any lower intensities in other sectors are then considered to be due to ion loss. Finally, the transmission is calculated by dividing the number of detected ions with a specific m/z by the highest ion count across the p-projection angle on the p_{yz} plane. In the case of N^+ and O^+ ions, which were overlapping with each other, we isolated the non-overlapping portion of the peak while keeping the nominal flight time the same. Subsequently, we doubled the detected ion count under the assumption that

an equivalent number of ions were present in the overlapping region. Then the ion transmission was estimated as described above. Using this approach, we were able to reliably estimate the transmission of all ions except for bromine-containing ions due to the overlapping isotopes.

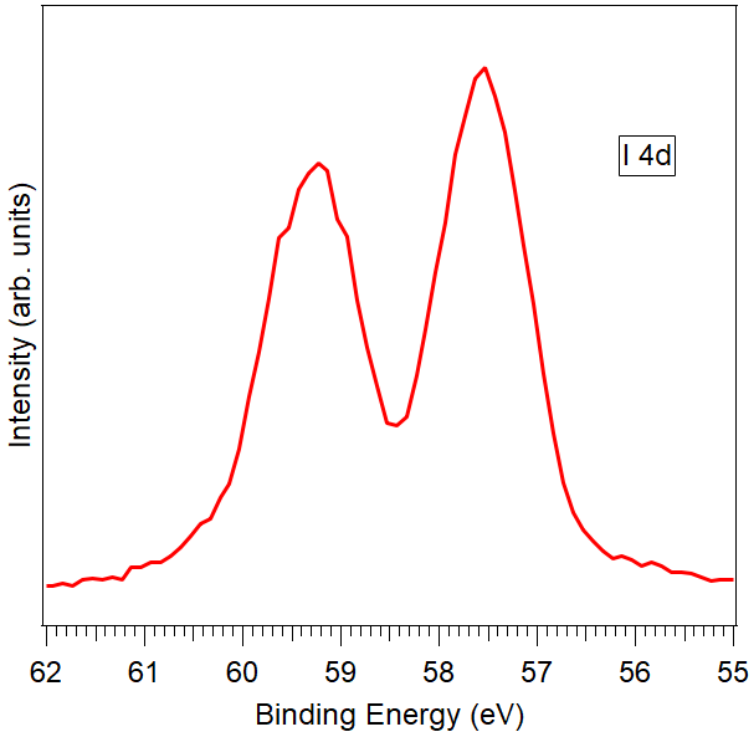

Figure S1.
I 4d photoelectron spectrum of BrINim measured at $hv = 85$ eV. The spectrum is extracted from the PEPIPICO data set.

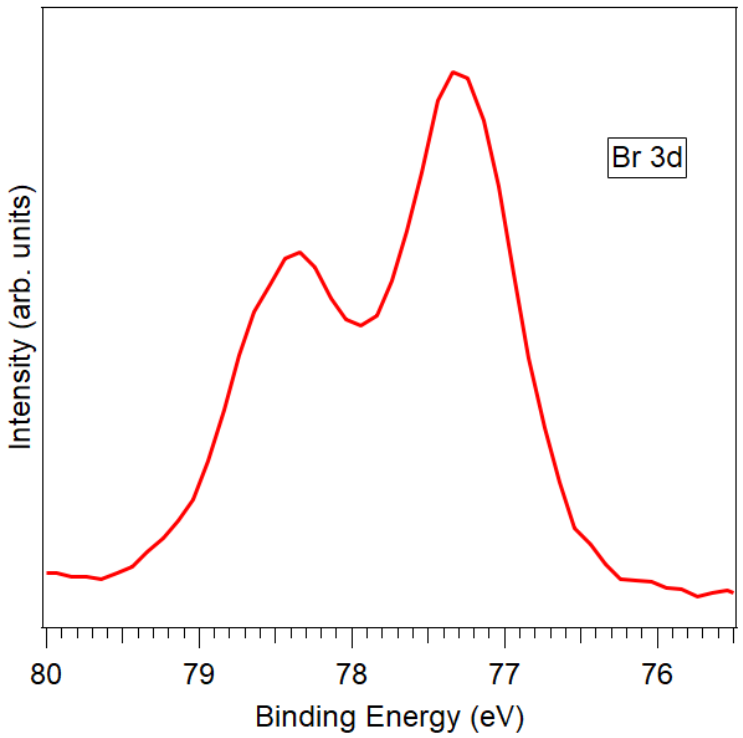

Figure S2.
Br 3d photoelectron spectrum of BrINim measured at $hv = 115$ eV. The spectrum is extracted from the PEPIPICO data set.

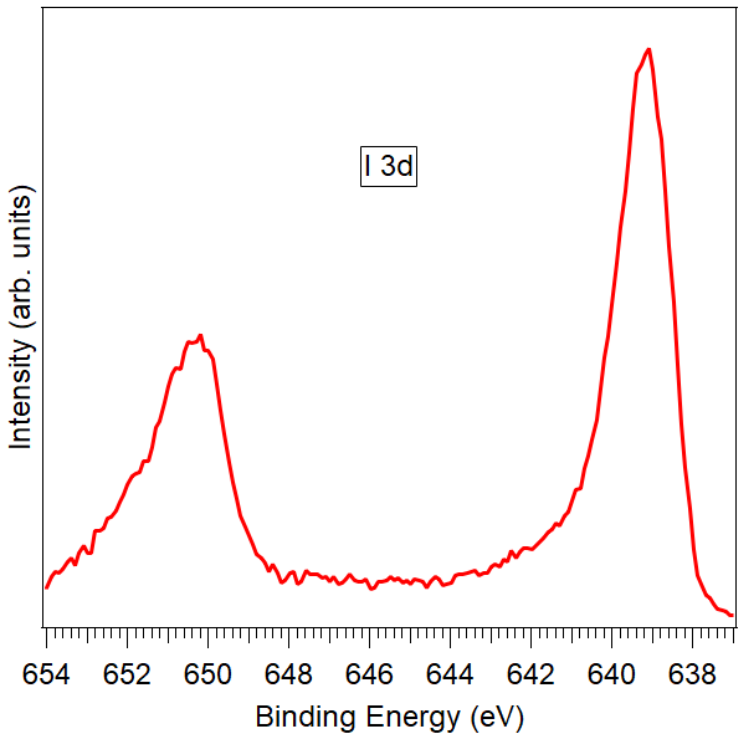

Figure S3.
I 3d photoelectron spectrum of BrINim measured at $hv = 670$ eV. The spectrum is extracted from the PEPIPICO data set.

Table SI. Ion transmission correction. In the table, experimentally determined peak areas are given in the Exp column, followed by the estimated transmission, T. Lost ions were then calculated and the total ion number (Exp+Lost ions) is presented in the SUM column. The percent shows the fraction of a particular ion normalized to the total ion count (100%).

	I 4d					Br 3d					I 3d				
m/z	Exp	T	Lost ions	SUM	%	Exp	T	Lost ions	SUM	%	Exp	T	Lost ions	SUM	%
7	0.00	1.00	0.00	0.00	0.00	0.00	1.00	0.00	0.00	0.00	0.00	0.68	0.00	0.00	0.11
8	0.00	1.00	0.00	0.00	0.00	0.00	1.00	0.00	0.00	0.00	0.01	0.64	0.00	0.01	0.50
12	0.02	0.75	0.01	0.02	1.15	0.05	0.79	0.01	0.06	3.64	0.26	0.70	0.11	0.37	20.04
13	0.01	0.55	0.01	0.01	0.54	0.01	0.68	0.00	0.01	0.61	0.00	1.00	0.00	0.00	0.00
14	0.00	0.46	0.00	0.00	0.21	0.01	0.70	0.00	0.01	0.60	0.15	0.61	0.10	0.25	13.57
16	0.02	0.72	0.01	0.03	1.65	0.05	0.63	0.03	0.08	4.76	0.12	0.42	0.17	0.29	15.49
24	0.01	0.79	0.00	0.01	0.50	0.01	0.74	0.00	0.02	1.03	0.03	0.78	0.01	0.04	2.29
26	0.00	1.00	0.00	0.00	0.00	0.00	1.00	0.00	0.00	0.00	0.09	0.63	0.05	0.14	7.44
27	0.06	0.47	0.07	0.14	6.47	0.09	0.50	0.09	0.18	10.64	0.00	1.00	0.00	0.00	0.00
30	0.37	0.78	0.10	0.47	22.55	0.28	0.82	0.06	0.34	19.68	0.06	0.87	0.01	0.07	3.63
38	0.19	0.73	0.07	0.27	12.67	0.16	0.70	0.07	0.22	13.08	0.06	0.72	0.02	0.09	4.78
41	0.01	0.50	0.01	0.03	1.32	0.01	0.38	0.02	0.03	1.89	0.01	0.70	0.01	0.02	1.04
46	0.09	0.87	0.01	0.11	5.00	0.04	0.88	0.01	0.05	2.76	0.01	0.49	0.01	0.01	0.71
53	0.06	0.82	0.01	0.07	3.56	0.04	0.73	0.02	0.06	3.59	0.01	0.81	0.00	0.01	0.78
64	0.00	1.00	0.00	0.00	0.00	0.00	1.00	0.00	0.00	0.00	0.02	0.54	0.02	0.03	1.86
65	0.04	0.63	0.02	0.07	3.14	0.02	0.63	0.01	0.04	2.27	0.03	0.45	0.04	0.08	4.04
80	0.16	1.00	0.00	0.16	7.52	0.24	1.00	0.00	0.24	13.78	0.17	1.00	0.00	0.17	9.35
92	0.05	1.00	0.00	0.05	2.58	0.05	1.00	0.00	0.05	3.15	0.01	1.00	0.00	0.01	0.64
107	0.05	1.00	0.00	0.05	2.31	0.03	1.00	0.00	0.03	1.76	0.01	1.00	0.00	0.01	0.27
118	0.04	1.00	0.00	0.04	1.94	0.03	1.00	0.00	0.03	1.78	0.02	1.00	0.00	0.02	0.98
127	0.29	0.72	0.11	0.40	19.13	0.19	0.81	0.05	0.24	13.94	0.16	0.73	0.06	0.23	12.12
139	0.02	0.69	0.01	0.03	1.44	0.01	0.66	0.01	0.02	1.03	0.00	0.55	0.00	0.01	0.34
145	0.02	1.00	0.00	0.02	0.93	0.00	1.00	0.00	0.00	0.00	0.00	1.00	0.00	0.00	0.00
154	0.02	0.50	0.02	0.04	1.70	0.00	1.00	0.00	0.00	0.00	0.00	1.00	0.00	0.00	0.00
166	0.03	0.41	0.04	0.07	3.41	0.00	1.00	0.00	0.00	0.00	0.00	1.00	0.00	0.00	0.00
192	0.00	1.00	0.00	0.00	0.14	0.00	1.00	0.00	0.00	0.00	0.00	1.00	0.00	0.00	0.00
246	0.00	1.00	0.00	0.00	0.16	0.00	1.00	0.00	0.00	0.00	0.00	1.00	0.00	0.00	0.00

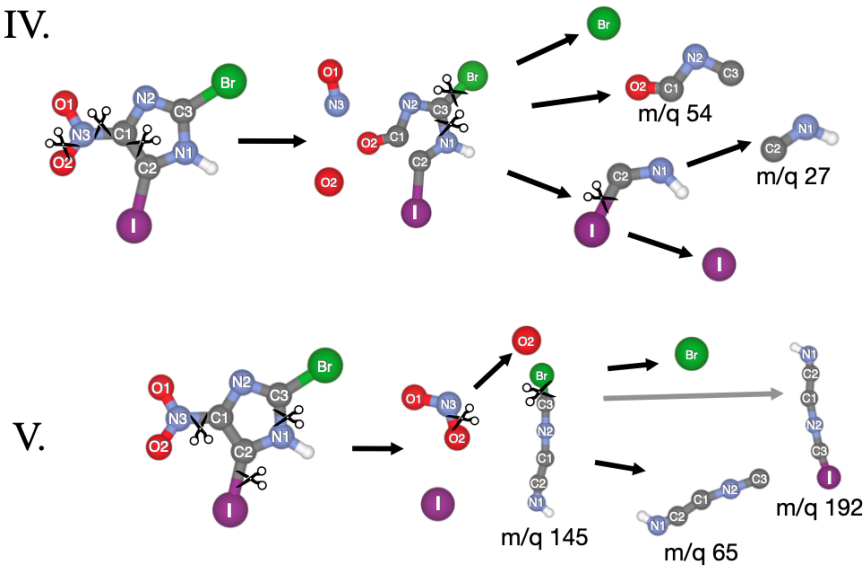

Figure S4. Two additional fragmentation pathways simulated for charge state q=+2. Path IV depicts the release of NO fragment while the opening of the ring causes the production of m/q 54 and m/q 27 (visible in the experiment). Path V shows a possible path for the production of fragment m/q 192 via recombination of m/q 65 with an iodine atom.